Effect of Heat Treatments on Hydrogen Environment Embrittlement of Alloy 718

Seiji FUKUYAMA and Kiyoshi YOKOGAWA

Chugoku National Industrial Research Institute, AIST, MITI, Japan

2-2-2 Hiro-Suehiro, Kure, Hiroshima, 737-01, Japan

Abstract

Tensile property and fatigue crack growth of Alloy 718, which was solution-annealed at 1223 ~ 1323 K and aged, were investigated in high-pressure hydrogen of 1.1 MPa up to 19.7 MPa and argon at room temperature up to 773 K. The effect of gaseous inhibitors added to hydrogen atmosphere on the fatigue crack growth was also investigated to prevent hydrogen assisted fatigue crack growth. Hydrogen environment embrittlement (HEE) increased with increasing δ phase and with decreasing testing temperature. HEE still occurred at 773 K. Delayed fracture was found predominantly in fatigue crack growth in hydrogen. The crack initiation occurred at carbide, then the crack propagated along the interface between δ phase and γ matrix of the alloy with δ phase or along the grain boundary of the alloy without δ phase. It was observed that oxygen or carbon monoxide added to hydrogen atmosphere had much effect to prevent hydrogen assisted fatigue crack growth.

Superalloys 718, 625, 706 and Various Derivatives
Edited by E.A. Loria
The Minerals, Metals & Materials Society, 1994

Introduction

Alloy 718 of Ni-base superalloy which is superior to the resistance to high temperature has been used for the main construction materials of the hydrogen fueled rocket engine of H-II rocket, LE-7[1] engine, developed by National Space Development Agency of Japan (NASDA). As the alloy is exposed to hydrogen in the engine, hydrogen environment embrittlement (HEE) could be the important problem for the alloy.

The effects of hydrogen on mechanical properties of the alloy were mainly investigated when National Aeronautics and Space Administration (NASA) developed the Space Shuttle Main Engine (SSME). The mechanical tests of Alloy 718 in high pressure hydrogen have been carried out by Harris, Jr. et al.[2] in Pratt and Whitney Aircraft and Walter et al.[3] in Rocketdyne Division which manufactured SSME. Furthermore Rie et al.[4] carried out low cycle fatigue tests of Alloy 718 in high pressure hydrogen. However the effect of metallic structure on HEE of the alloy has not been clear yet.

In the present paper, tensile tests and fatigue crack growth tests of the alloy were carried out in high pressure hydrogen of 1.1 MPa up to 19.7 MPa and argon at room temperature up to 773 K. The effect of the heat treatment on HEE of the alloy was discussed. The effect of inhibitive gas added to hydrogen atmosphere to prevent hydrogen assisted fatigue growth was also discussed.

Experimental Procedure

Material

The materials used were Alloy 718 whose chemical compositions in wt % are shown in **Table I**. These materials were casted, hot forged and treated with the following heat treatment. The material was solution-annealed at the temperature range from 1223 K up to 1333 K for 3.6 ks, and then oil-quenched. The annealed materials were aged at 991 K for 28.8 ks, cooled at a rate of 1.5×10^{-2} K/s, aged at 894 K for 36.0 ks to precipitate γ' and γ'', and then cooled in air.

Metallographic structure of the heat treated alloy by using a scanning electron microscope are shown in **Fig. 1**. Microstructures of the alloy solution-annealed at 1233 K consisted of the large carbide particles of precipitate (A), continuous δ phase (B), a needle-shaped precipitate of δ phase in the Widmanstaetten pattern (C) and a matrix. Precipitates of γ' and γ'' were formed throughout the structure during the aging treatment and were not observed at the magnifications used, however the matrix consisted of γ, γ' and γ'' characterized by using transmission electron microscope. Furthermore, microstructure of the alloy solution-annealed at 1323 K consisted of the large carbide (A) and a matrix.

Table I Chemical compositions of Alloy 718

Materials	C	Si	Mn	P	S	Ni	Cr	Mo	Co	Al	Ti	Cu	Fe	B	Cb+Ta
Alloy(A)	0.03	0.06	0.16	0.002	0.001	51.95	18.76	3.02	0.06	0.42	1.02	0.02	Rem.	0.006	5.06
Alloy(B)	0.05	0.05	0.13	0.005	0.005	52.00	18.89	3.04	0.05	0.48	1.15	0.05	Rem.	0.004	5.32

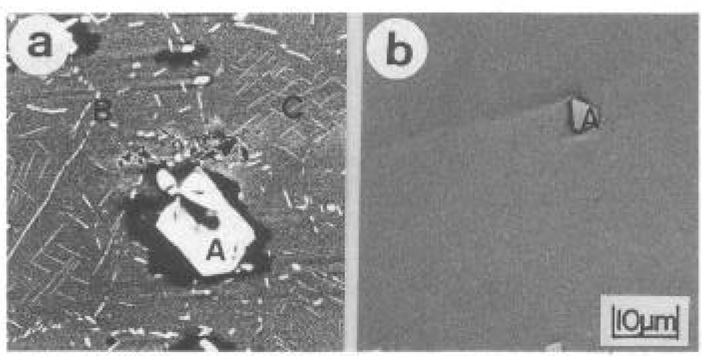

Fig. 1 Metallographic structures of Alloy 718.
(a):Solution-annealed at 1243 K (A:Nb-Ti carbide, B:δ phase, C:δ phase of Widmanstaetten structure.), (b):Solution-annealed at 1323 K (A:Nb-Ti carbide.)

Tensile Testing

Cylindrical tensile specimens with a gauge section of 20 mm long and 4 mm in diameter were machined from the heat treated materials (A). The surface of the specimens were polished with 0.05 μm γ- Al_2O_3 dispersed on microcloth and washed in an acetone bath. Tensile tests were conducted with a strain rate of 4.17×10^{-5} s^{-1} by using a specially designed apparatus[5]. The tests were conducted in 1.1 MPa argon of 99.99 % and 19.7 MPa hydrogen of 99.9999 % purity. The tests were performed at 293 K up to 773 K.

Fatigue Crack Growth Testing

DCB type specimens with 107 mm in width and 10 mm in thickness were machined from the heat treated materials (B). The fatigue crack growth tests were conducted in 1.1 MPa argon, and 1.1 MPa and 19.7 MPa hydrogen by using a specially designed fatigue testing apparatus[6,7] under the conditions of sinusoidal tension-tension cycle from 0.01 to 10 Hz with a stress ratio R=0.1. Crack length was monitored by means of the AC electric-potential technique. All tests were performed at 293±1 K. K of the DCB type of specimen was calculated by the following equation:

$$K = (\mathbf{P}/H(\mathbf{a})^{1/2})(\mathbf{a}/H(\mathbf{a})+0.7)\cdot f(\mathbf{m})$$ [8]

where **P** is the load per unit effective thickness[9], **a** is the crack length, H(**a**) is the beam height at **a**, **m** is the gradient of the beam, and f(**m**) is a constant of 2.98 in this case.

Gaseous Inhibitors

The fatigue crack growth tests were also conducted in 1.1 MPa hydrogen gas containing gaseous inhibitors. The kinds of gaseous inhibitors tested and the concentration in pure hydrogen gas (99.9999 %) were as follows; oxygen (0.19 %), carbon monoxide (0.99 %), carbon dioxide (1.01 %) or water vapor (0.03 %). The hydrogen containing each inhibitor was provided by the gas supplier. All tests were performed at 293±1 K.

Results and Discussion

Tensile Properties

Effect of Temperature of Solution Treatment. The effect of temperature of the solution treatment on the tensile properties of the alloy in 1.1 MPa argon and 19.7 MPa hydrogen is shown in **Fig.2**. 0.2 % proof stress (PS) and ultimate tensile strength (UTS) both in argon and hydrogen decreased, and elongation and reduction of area increased with increasing temperature of the solution treatment. Elongation and reduction of area were almost constant above 1273 K. Hydrogen showed marked effect on UTS and ductility. UTS, elongation and reduction of area in hydrogen were smaller than those in argon. UTS, elongation and reduction of area of the alloy for the solution-annealed at 1233 K in hydrogen was 98 %, 33 % and 31 % of that in argon respectively. While in hydrogen UTS, elongation and reduction of area of the alloy solution-annealed at 1323 K was 100 %, 41 % and 47 % of that in argon respectively. The effect of hydrogen on UTS, elongation and reduction of area increased with decreasing temperature of the solution treatment, so that the effect of hydrogen on the tensile properties increased with increasing δ phase. However hydrogen shows no effect on PS.

Fracture surfaces of the alloy fractured in 19.7 MPa hydrogen at room temperature are shown in **Fig.3**. The crack initiation occurred at carbide. Intergranular fracture and brittle transgranular fracture were observed on the fracture surface of the alloy without δ phase. The brittle transgranular fracture along the interface between δ phase and γ matrix were mainly observed on the fracture surface of the alloy with δ phase. Dimple rupture were mainly observed on the fracture surface of the alloy both with and without δ phase in argon. Dimple size of the alloy without δ phase was smaller than that with δ phase.

Effect of Testing Temperature. The effect of testing temperature on HEE of the alloy solution-annealed at 1323 K (without δ phase) is shown in **Fig.4**. PS and UTS in argon decreased with increasing temperature, and elongation and reduction of area were almost constant independently of temperature. While PS and UTS in hydrogen decreased with increasing temperature, however elongation and reduction of area increased with increasing temperature.

It is found that HEE still occurred at 773 K. The effect of testing temperature on tensile properties of the alloy with δ phase both in argon and hydrogen showed similar tendency of the alloy without δ phase. The effect of testing temperature on HEE of the alloy with δ phase also showed similar tendency of the alloy without δ phase.

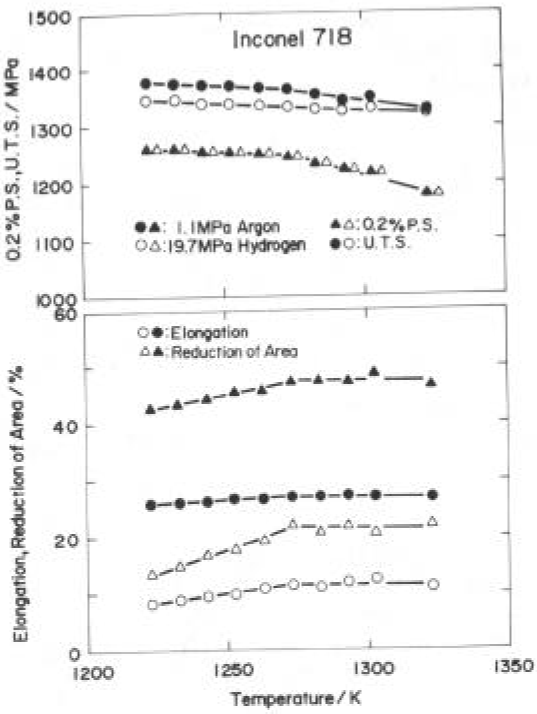

Fig.2 Effect of temperature of solution treatment on tensile properties of Alloy 718 in 1.1 MPa argon and 19.7 MPa hydrogen at 293 K.

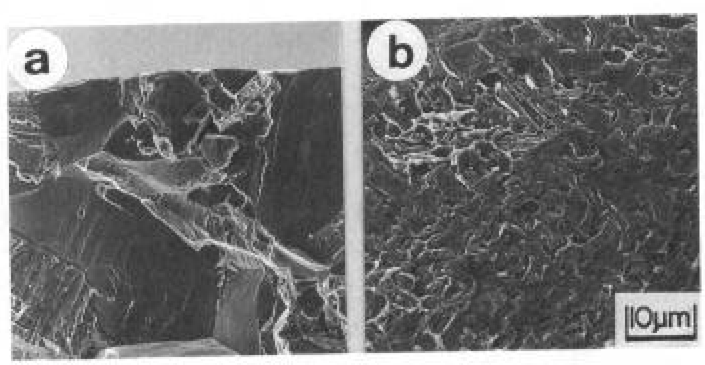

Fig.3 Fracture surfaces of Alloy 718 fractured in 19.7 MPa hydrogen at 293 K. (a) : without δ phase, (b) : with δ phase

Dimple rupture was mainly observed on the fracture surface of the alloy both with and without δ phase in argon at elevated temperatures. While the step like pattern was mainly observed on the fracture surface of the alloy both with and without δ phase in hydrogen at elevated temperatures. The step like pattern of the alloy with δ phase in 19.7 MPa at 573 K is shown in **Fig.5**.

Fatigue Crack Growth

Effect of ΔK. The effect of stress intensity factor range (ΔK) on fatigue crack growth rate (da/dN) of the alloys is shown in **Fig.6**. The alloy solution-annealed at 1323 K (without δ phase) and that solution-annealed at 1243 K (with δ phase) were used in the figure. da/dN of all the alloys increased with increasing ΔK. Hydrogen showed significant effect on da/dN of the alloy with δ phase above ΔK of 35 MPa•m$^{1/2}$. da/dN in hydrogen was higher than that in argon, i.e. da/dN in argon was 1.8×10^{-7} m/cycle at ΔK of 50 MPa•m$^{1/2}$, while that in hydrogen was 2.7×10^{-7} m/cycle, so that da/dN in hydrogen is 1.5 times higher than that in argon. However hydrogen showed little effect on da/dN below ΔK of 35 MPa•m$^{1/2}$. Hydrogen showed a little effect on da/dN of the alloy without δ phase. da/dN of the alloy with δ phase was higher than that of the alloy without δ phase, so that fatigue crack growth increases by δ phase both in argon and hydrogen, and the effect of hydrogen on da/dN increases by δ phase.

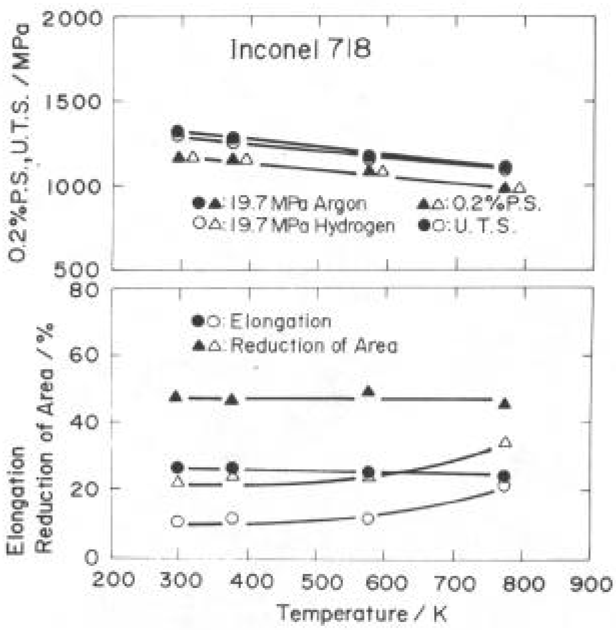

Fig.4 Effect of testing temperature on hydrogen environment embrittlement of Alloy 718 without δ phase.

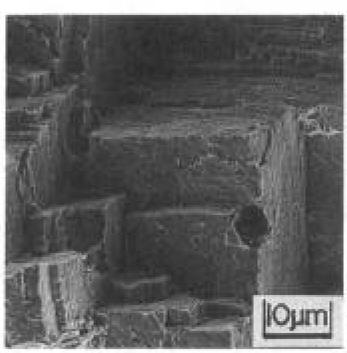

Fig.5 Fracture surface of Alloy 718 with δ phase fractured in 19.7 MPa hydrogen at 573 K.

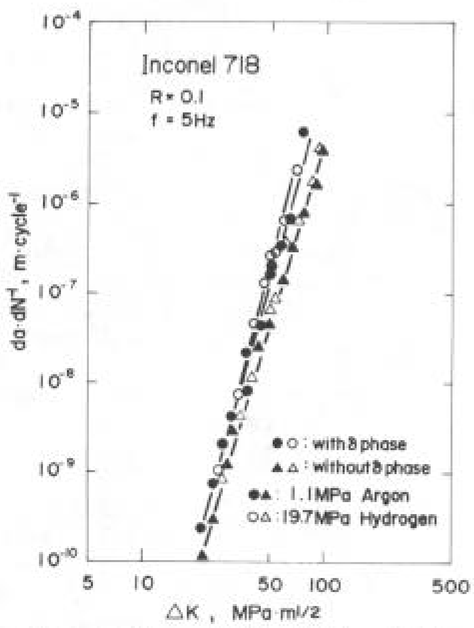

Fig.6 Effect of ΔK on da/dN of Alloy 718 in 1.1 MPa argon and 19.7 MPa hydrogen at 293 K.

Effect of Frequency. The effect of **f** on da/dN of the alloy without δ phase is shown in **Fig.7**. da/dN in argon was almost constant, while that in hydrogen increased with decreasing **f** and with increasing hydrogen pressure. da/dN in 19.7 MPa hydrogen at **f**=1 Hz is 1.3 times higher than that in argon, while that at **f**=0.1 Hz is 3.7 times higher and that at **f** = 0.01 Hz is 23 times higher, so that the effect of hydrogen on da/dN increases with decreasing **f**.

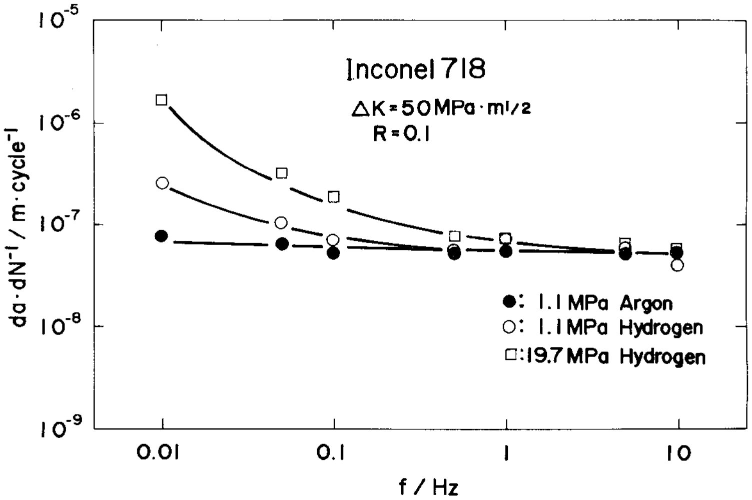

Fig.7 Effect of **f** on da/dN of Alloy 718 without δ phase in 1.1 MPa argon, and 1.1 and 19.7 MPa hydrogen.

It is proposed by Wei et al.[10] that the rate of fatigue crack growth in an aggressive environment, (da/dN)e, is composed of the sum of three components,

$$(da/dN)e=(da/dN)r+(da/dN)cf+(da/dN)scc$$

where (da/dN)r is the rate of fatigue crack growth in an inert environment, (da/dN)scc is the contribution by sustained-load crack growth at K levels above K_{ISCC} and (da/dN)cf represents a cycle-dependent contribution requiring synergistic interaction of fatigue and environmental attack. In the model, (da/dN)scc depends on time.

$$(da/dN)e=(da/dN)r+(da/dN)cf+\int \tau\,(da/dt)scc\,dt$$
$$(da/dt)e=\mathbf{f}\,[(da/dN)r+(da/dN)cf]+(da/dt)scc$$

The effect of **f** on da/dt of the alloy without δ phase is shown in **Fig.8**. da/dt in argon decreased with decreasing **f**. While da/dt in 19.9 MPa hydrogen decreased with decreasing **f** down to 0.5 Hz and that in 1.1 MPa hydrogen decreased with decreasing **f** down to 0.1 Hz, and then were almost constant. These results showed that delayed fracture was predominantly in fatigue crack growth in hydrogen at lower **f**.
Walter et al.[3] studied the fatigue crack growth of Alloy 718. The metallic structure of the alloy consisted of the carbides and γ matrix only. Fatigue crack growth test was conducted in hydrogen up to 68.9 MPa under the conditions of tension-tension cycle from 0.1 to 1 Hz with a stress ratio R = 0.1. da/dN in hydrogen was higher than that in helium in their results. They also studied the effect of **f** on da/dN under the condition of **f** from 0.1 to 1 Hz under ΔK of 55 MPa•m$^{1/2}$ and found that da/dN in hydrogen increased with decreasing **f**. da/dN in hydrogen was 5 times higher than that in helium at 1 Hz. However they conducted the test in helium at 1 Hz only, so that the effect of hydrogen on fatigue crack growth was not clear thoroughly.

Fracture surfaces. The fracture surfaces of the alloy without δ phase at f = 5 Hz in 1.1 MPa argon and 19.7 MPa hydrogen are shown in **Fig.9**. The plate like fracture formed along the slip plane[11] was observed on the fracture surface both in argon (a) and hydrogen (b) at lower ΔK. Striations were observed on the fracture surface in argon (c) at ΔK of 50 MPa•m$^{1/2}$. while brittle transgranular fracture was mainly surface in hydrogen (d).
The fracture surfaces of the alloy with δ phase at f = 5 Hz in 1.1 MPa argon and 19.7 MPa hydrogen are shown in **Fig.10**. The plate like fracture was also observed on the fracture

surface both in argon (a) and hydrogen (b) at lower ΔK. Both striations and transgranular fracture were observed on the fracture surface in argon (c) at ΔK of 50 MPa•m$^{1/2}$, while brittle transgranular fracture along the interfaces between δ phase and γ matrix was mainly observed in hydrogen (d).

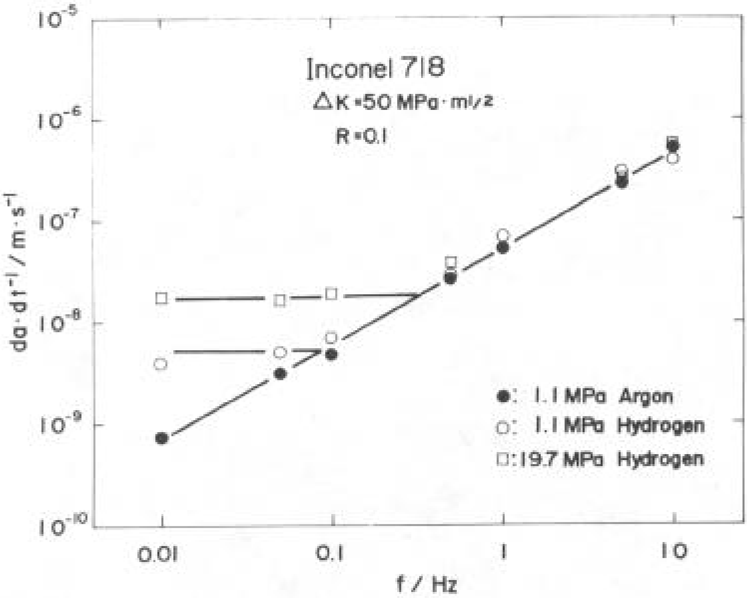

Fig.8 Effect of **f** on da/dt of Alloy 718 without δ phase in 1.1 MPa argon, and 1.1 and 19.7 MPa hydrogen.

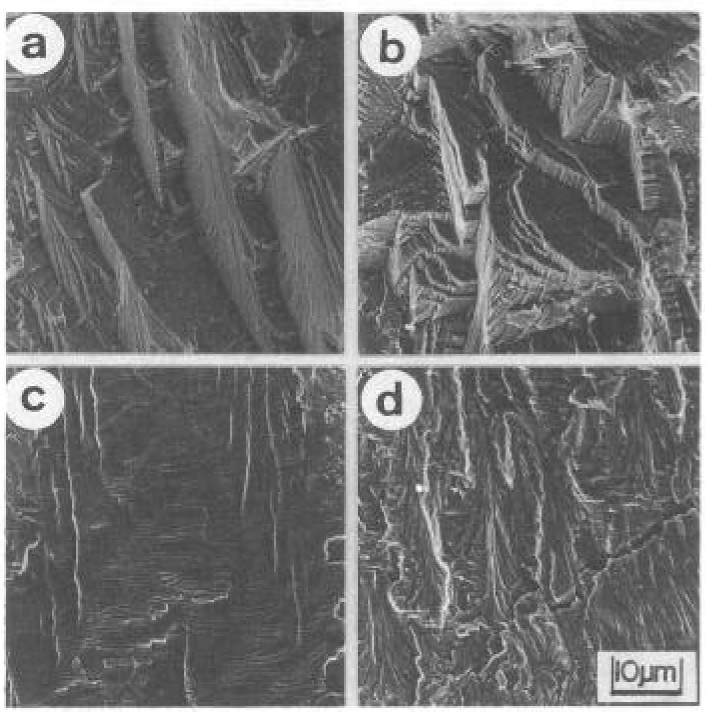

Fig.9 Fracture surfaces of Alloy 718 without δ phase at f=5 Hz in 1.1 MPa argon and 19.7 MPa hydrogen. (a,b) : at ΔK of 30 MPa•m$^{1/2}$, (c,d) : at ΔK of 50 MPa•m$^{1/2}$, (a,c) : in 1.1 MPa argon, (b,d) : in 19.7 MPa hydrogen

The effect of ΔK on fracture mode of the alloy in argon and hydrogen is shown in **Fig.11**. On the fracture surface of the alloy without δ phase in argon, the plate like fracture decreased and the brittle transgranular fracture increased with increasing ΔK below ΔK of 35 MPa•m$^{1/2}$. Striations were observed above ΔK of 35 MPa•m$^{1/2}$ and the dimple rupture was also observed above ΔK of 63 MPa•m$^{1/2}$. While in hydrogen, the plate like fracture decreased with increasing

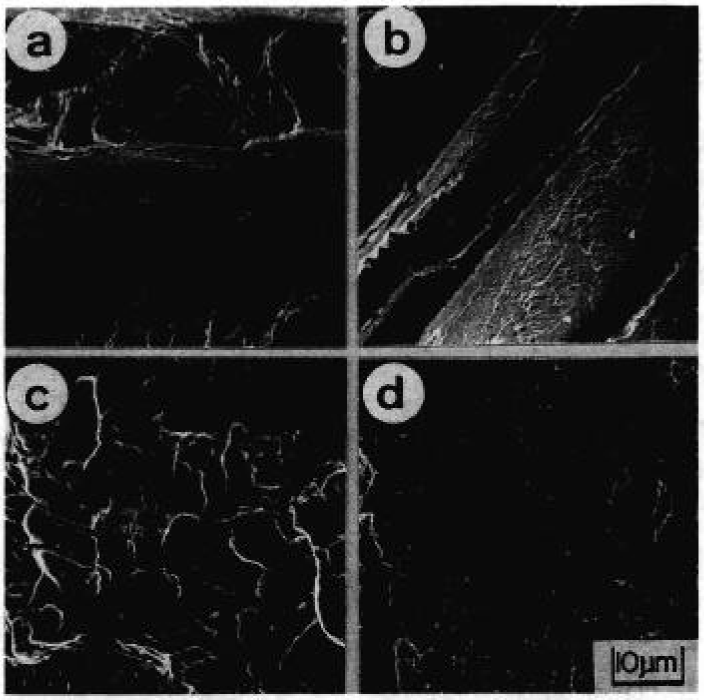

Fig.10 Fracture surfaces of Alloy 718 with δ phase at f=5 Hz in 1.1 MPa argon and 19.7 MPa hydrogen. (a,b) : at ΔK of 30 MPa•m$^{1/2}$, (c,d) : at ΔK of 50.MPa•m$^{1/2}$, (a,c) : in 1.1 MPa argon, (b,d) : in 19.7 MPa hydrogen

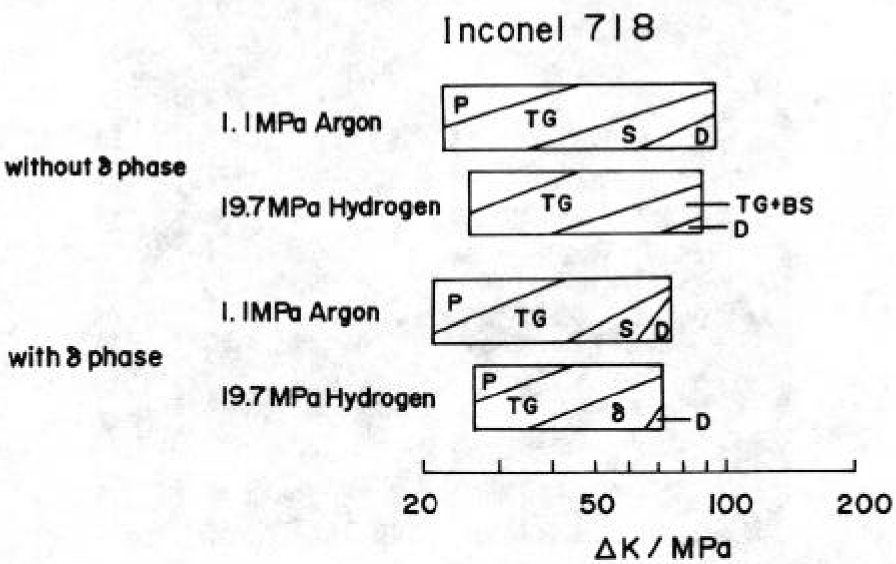

Fig.11 Effect of ΔK on fracture mode of Alloy 718 in 1.1 MPa hydrogen and 19.7 MPa hydrogen. P : Plate like fracture, TG : Transgranular fracture, S : Striation, BS : Brittle striation, D : Dimple rupture, δ : Fracture along the δ phase.

ΔK below ΔK of 47 MPa•m$^{1/2}$ as like as that in argon. The brittle transgranular fracture increased with increasing ΔK below 47 MPa•m$^{1/2}$. The dimple rupture was also observed above ΔK of 71 MP•m$^{1/2}$.

On the fracture surface of the alloy with δ phase in argon, the plate like fracture decreased and the brittle transgranular fracture increased with increasing the ΔK below ΔK of 44 MPa•m$^{1/2}$. Striations were observed above ΔK of 44 MPa•m$^{1/2}$ and dimple rupture was also observed at ΔK of 63 MPa•m$^{1/2}$. While in hydrogen, the plate like fracture increased with increasing ΔK below the ΔK of 45 MPa•m$^{1/2}$ as like as that in argon. The brittle transgranular fracture along the interface between δ phase and γ matrix increased with increasing ΔK above 35 MPa•m$^{1/2}$. The dimple rupture was also observed above ΔK of 65 MPa•m$^{1/2}$.

On the basis of the results, hydrogen showed a marked effect on the fatigue crack growth above ΔK which ductile striations were formed on the fracture surface in argon. It is well known that the tensile ductile striations have large plastic zone at the crack tip[12,13,14]. It was found that hydrogen reduced the tensile ductility. As the crack growth occurred before the ductile striations were formed with large plastic deformation in hydrogen, so that the crack growth in hydrogen was higher than that in argon.

Prevention of Hydrogen Assisted Fatigue Crack Growth

The effect of gaseous inhibitors added to 1.1 MPa hydrogen on the fatigue crack growth of the alloy is shown **Fig.12**. The inhibitive effect is expressed as

$$[(da/dN)\text{Inhibitor} - (da/dN)\text{Argon}] \;/\; [(da/dN)\text{Hydrogen} - (da/dN)\text{Argon}]$$

It was found that the addition of oxygen or carbon monoxide had much effect on preventing hydrogen assisted fatigue crack growth, but that of carbon dioxide had little effect. The authors[15,16] also found that oxygen or carbon monoxide showed much effect for steels.

According to the HEE theory[17], hydrogen is adsorbed on the metal surface and penetrates into the metal body, and then hydrogen embrittlement comes about. It is expected that some compounds whose adsorption on metal surface is stronger than that of hydrogen would retard HEE. Adsorption of oxygen and carbon monoxide on metal are stronger than that of hydrogen[18], so that it is expected that their addition to hydrogen atmosphere retards hydrogen assisted fatigue crack growth.

On the other hand, it is found that water vapor accelerated the fatigue crack growth of the alloy. The authors[16] found that water vapor accelerated the fatigue crack growth of 2.25Cr-1Mo steel. The process is considered as follows; the chemical reaction between the metal and water vapor occurred on the fracture surfaces at the crack tip of the alloy, and then hydrogen came out. It is well known that hydrogen in nascent state[19] accelerates hydrogen embrittlement. So, water vapor accelerated the fatigue crack growth.

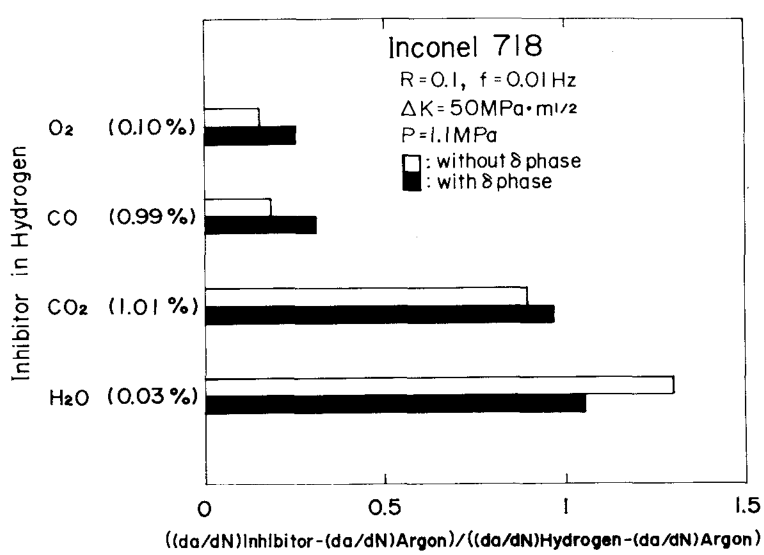

Fig.12 Effect of gaseous inhibitors added to 1.1 MPa hydrogen on fatigue crack growth of Alloy 718.

Conclusion

Tensile and fatigue crack growth testings of Alloy 718 were conducted in high-pressure hydrogen of 1.1 MPa up to 19.7 MPa and argon at room temperature up to 773 K. Effects of heat treatments on HEE of the alloy were investigated. The effect of gaseous inhibitors added to hydrogen atmosphere on the fatigue crack growth of the alloy was also investigated to prevent hydrogen assisted fatigue crack growth. The results obtained are as follows;

(1) Effect of hydrogen on the tensile property increased with increasing δ phase and with decreasing testing temperature. HEE still occurred at 773 K. The crack initiation occurred at carbide, and then the crack propagated along the interface between δ phase and γ matrix of the alloy with δ phase or along the grain boundary of the alloy without δ phase.

(2) Hydrogen showed marked effect on the fatigue crack growth above the ΔK which the striations were formed on the fracture surface in argon. Effect of hydrogen on the fatigue crack growth increased with decreasing the frequency of the cyclic loading. Delayed fracture was found predominantly in fatigue crack growth in hydrogen.

(3) It was observed that oxygen or carbon monoxide added to hydrogen atmosphere had much effect to prevent hydrogen assisted fatigue crack growth.

Acknowledgement

This study is supported financially by the Agency of Industrial Science and Technology, MITI, as New Energy R/D Grants in 1993.

References

1. Y.Yamada and E. Sogame, PISSTA787, 1987, 628.
2. J. A. Harris, Jr. and M. C. VanWanderham, NASA CR-124394, 1973.
3. R. J. Walter and W. T. Chandler, NASA CR-124410, 1973.
4. K. Rie, J. Ruge and W. Kohler, " Low-cycle Fatigue of Fe-Cr-Ni-Austenite and Ni-base Alloys in High Pressure Hydrogen," Proceedings JIMIS-2, Hydrogen in Metals, 1980, 529
5. K. Yokogawa S. Fukuyama, M. Mitsui and K. Kudo, "Pressure Vessel for Tensile Testing in High-Pressure Gases at Elevated Temperature," Rev. Sci. Instrum., **Vol. 53**, 1978, 50.
6. S. Fukuyama, K. Yokogawa and M. Araki, " Fatigue Crack Growth of AISI4340 Steel in High Pressure Hydrogen at Room Temperature," J. Soc. Mater. Sci. Jpn (Japan), **Vol.34**, 1985, .
7. S. Fukuyama, K. Yokogawa, K. Kudo and M. Araki, " Fatigue Properties of Type 304 Stainless Steel in High Pressure Hydrogen at Room Temperature," Trans. Jpn. Inst. Met., **Vol.26**, 1985, 325.
8. H. Okamura, (Senkei Hakai Rikigaku Nyumon (Japan)), Baifukan, 1976, 220.
9. The Japan Society of Mechanical Engineering, (Standard Method of Test for Elastic-Plastic Fracture Toughness J_{IC} (Japan)), JSME S001-1981, 1981.
10. R. P. Wei and G. W. Simmons, (Fatigue : Environment and Temperature Effects) Edited by John J. Burke and Volker Weiss, PLENUM PRESS, 1983, 59.
11. M. Clavel and A. Pineau, " Frequency and Wave-Form Effect on the Fatigue Crack Growth Behavior of Alloy 718 at 298 K and 823 K," Met. Trans., **Vol.9A**, 1978, 471.
12. J. F. Knott, Translated into Jpn. by H. Miyamoto, (Hakairikigaku no Kiso), Baifukan, 1977, 122.
13. R. Koterazawa, (Fractography To Sono Ouyou (Japan)), Nikkankogyo shinbunsha, 1981, 47.
14. H. Kobayashi, K. Hirono, H. Kayakabe and H. Nakazawa, " Influence of Hydrogen on Fracture Toughness of High Strength Steels," 5th International Conference of Fracture, Cannes, France, Fracture Research Advances IV, **Vol.4**, 1981, 1909.
15. S. Fukuyama, K. Yokogawa and M. Araki, " Fracture Toughness and Fatigue Crack Growth of AISI4340 Steel in High Pressure Hydrogen at Room Temperature," Proceedings of 6th International Conference on Pressure Vessel Technology, Beijing, China, Pergamon Press, **Vol. 2**, 1988, 539.
16. S. Fukuyama, K. Yokogawa, " Prevention of Hydrogen Environmental Assisted Crack Growth of 2.25Cr-1Mo Steel by Gaseous Inhibitors," Proceedings of 7th International Conference on Pressure Vessel Technology, Dusseldorf, German, VdTUV, **Vol. 2**, 1992, 914.
17. H. R. Gray, (Hydrogen Embrittlement Testing), ASTM STP543, American Society for Testing and Materials, 1974, 133.
18. Catalysis Soc. Jpn., (Shokubai Koza **Vol. 1** (Japan)), Kodansha Scientific, 1985, 41.
19. Jpn. Inst. Metals, (Kinzoku Binran (Japan)), Marzen, 1971, 1625.